IEEE Access
Multidisciplinary ⋮ Rapid Review ⋮ Open Access Journal

Received 17 February 2024, accepted 29 February 2024, date of publication 4 March 2024, date of current version 11 March 2024.

Digital Object Identifier 10.1109/ACCESS.2024.3373043

RESEARCH ARTICLE

Rank Exponent Method Based Optimal Control of AGC for Two-Area Interconnected Power Systems

MAMTA[1], (Student Member, IEEE), V. P. SINGH[1], (Senior Member, IEEE), AKANKSHA V. WAGHMARE[1], (Student Member, IEEE), VEERPRATAP P. MEENA[2], (Member, IEEE), FRANCESCO BENEDETTO[3], (Senior Member, IEEE), AND TARUN VARSHNEY[4], (Senior Member, IEEE)

[1]Department of Electrical Engineering, Malaviya National Institute of Technology Jaipur, Jaipur 302017, India
[2]Department of Electrical and Electronics Engineering, Amrita School of Engineering, Amrita Vishwa Vidyapeetham, Bengaluru 560035, India
[3]SP4TE—Signal Processing for Telecommunications and Economics Laboratory, Economics Department, University of Roma Tre, 00145 Rome, Italy
[4]Department of Electrical Electronics and Communication Engineering, Sharda University, Greater Noida, Uttar Pradesh 201310, India

Corresponding authors: Francesco Benedetto (francesco.benedetto@uniroma3.it), Veerpratap P. Meena (vmeena1@ee.iitr.ac.in), and Tarun Varshney (tarun.varshney@sharda.ac.in)

ABSTRACT Automatic generation control (AGC) is employed in power systems to maintain balance between generation and load by adjusting output of generators in real time. Controller continuously monitors system frequency and tie-line power flow by responding to fluctuations in electricity demand and supply and optimizes generator dispatch, reduces power imbalances, and enhances grid stability. This work proposes and solves the issues of the AGC in two-area interconnected power systems by proposing a new approach based on both Jaya algorithm and the rank exponent method. In particular, we design a proportional-integral-derivative controller with derivative filtering (PIDm), where the effect of the noise is mitigated by the use of a filter with derivative gain. We propose to build the objective function, to tune the controller's parameters, as the linear combination of three sub-objectives, namely integral of time multiplied absolute error (ITAE) for frequency deviations, tie-line power deviation, and area-control errors (ACEs). The rank method is exploited to evaluate the weights of these sub-objectives, while the final overall objective function is minimized exploiting the Jaya algorithm. The proposed controller's performance is assessed in six different scenarios with load disturbances, and its effectiveness is compared to state-of-art controllers tuned using salp swarm algorithm (SSA), Nelder-Mead simplex (NMS), symbiotic organisms search (SOS), elephant herding optimization (EHO), and Luus-Jaakola (LJ) optimization algorithms. To illustrate the frequency and tie-line power changes, results are also shown, and a statistical study is finally carried out to evaluate the recommended controller's overall effectiveness. Additionally, Friedman rank test as no-parametric statistical analysis is also done in order to evaluate the significance level of optimization algorithms. Our numerical findings evidence that the proposed PIDm controller outperforms other existing optimization-based controllers in terms of performance and utility, thus proving to be very effective for handling AGC issues in two-are interconnected power systems.

INDEX TERMS Rank exponent method, AGC, Jaya optimization, interconnected power system.

I. INTRODUCTION

In power system, load demand is constantly varying. To meet out the increasing demand for power, single-area power systems are less reliable. Reliability is the main concern in operation of a power system. To ensure the reliability of power system, distinct areas' generators are interconnected via tie-lines. This type of interconnection is known as interconnected power system (IPS) [1]. In IPS, it is essential to operate all generators at the same frequency in a synchronized manner. The frequency of IPS will deviate from its nominal value whenever load variations in any area occur.

The associate editor coordinating the review of this manuscript and approving it for publication was K. Srinivas.

This issue is solved by adopting the concept of automatic generation control (AGC) [2]. The term AGC in power system operation is described as the variation of output electrical power from electric generators in a designated area whenever frequency of system, tie-line power, or both varies. AGC is required in power systems because of the following factors:

- Optimal scheduling of generators.
- To achieve minimum frequency deviation in interconnected power systems.
- To minimize the power deviation in tie lines.

A review of the literature reveals that various studies have been conducted on AGC in different power system setups. These studies encompass single-area (SA) power system [3], [4], two-area power system [5], [6], [7], and multi-area (MA) power system [8], [9], [10], [11]. The design and implementation of centralized and decentralized AGC controllers in two-region linked power systems with many power plants in each area with a PID structure are shown in [12]. In [7], an unregulated power setting, incorporating energy storage unit, is analysed by explaining the application, design, and assessment of a novel type of optimal controller (OC) for AGC of interconnected electrical power system, spanning two areas. The authors incorporate wind power generators (WPG) and solar power generators (SPG) as supplementary power sources within the AGC framework. This is delineated as a two-area thermal hybrid power generation system in [13], where thermal generation units are distributed across both regions, featuring WPG and SPG in area 1 and area 2. Additionally, in [14], the authors explore the influence of doubly fed induction generator (DFIG) on a conventional two-area power system comprising gas, hydro, and thermal power plants. In [15], a thermal-hydro power system is used to demonstrate AGC problem of three-area linked power systems including or excepting the presence of high voltage direct current (HVDC) connection. In [16], a four-area concept is taken into consideration for AGC of networked thermal systems using demand side management (DSM) in conjunction with automated voltage control (AVR).

Authors in [17] explore the automated load-frequency regulation of two-area interconnected power system using a novel fuzzy gain scheduling of a PI controller (FGPI). In [18], a genetic algorithm has been implemented to optimize the PID controller parameters for two-area power system with non-linearities in generation. Integral (I), proportional integral (PI), integral derivative (ID), proportional integral derivative (PID), and integral double derivative (IDD) are some of traditional controllers that authors in [19] proposed for dealing with AGC in a multi-area power system. The majority of research articles deal with PID controllers or their alternatives to handle AGC problems because of their simple and intuitive construction [20], [21].

The formulation of objective function plays a prime role in optimal tuning of controller parameters. Based on integral criterion, integral of squared error (ISE) [22], [23], integral of time multiplied absolute error (ITAE) [24], [25], integral of absolute error (IAE) [26], [27], and integral of time multiplied square error (ITSE) [24], [25], are used to formulate objective functions.

Area control errors (ACEs), tie-line power variations, and frequency deviations of interconnected areas are acknowledged as sub-objectives to frame objective function. Their weights determine the relative importance of sub-objectives in the overall objective function. To design an effective objective function, a systematic approach is essential to establish appropriate weights for the sub-objectives [28].

Due to load demand variability, traditional PID controllers often require specific tuning for efficient operation, making it challenging to maintain system stability across varying operating conditions in the nonlinear AGC environment. The adaptive backstepping scheme by incorporating entirely coupled recurrent neural network is implemented by Kumar et al. [29] to estimate the control terms. In literature, nonlinear control approach for thyristor-controlled series capacitors is also proposed for active power transfer by improving transient stability and voltage regulation of the power system in [30] by Fathollahi et al. Some of the researchers [31] presented the work on fractional control design are also available for improving transient stability and voltage regulation of the power system by adapting non-linear control design. In addition to this, some of the work on intelligent control design for power system applications are also presented by researchers in the literature [32], [33], [34].

In [35], various techniques are employed for tuning parameters of controller, including rule-based [36], meta-heuristic [37], and model-based tuning [38]. Recently, metaheuristic-based tuning [39] is employed for optimizing the parameters of controllers because of its better performance characteristics than rule-based and model-based tuning methods. Genetic algorithm [26], [40], bacteria foraging optimization [41], gravitational search algorithm [42], [43], grey wolf optimizer (GWO) [44], [45], [46], whale optimization [23], bat algorithm [47], [48], firefly algorithm [49], particle swarm optimization (PSO) [27], [50], artificial bee colony [51], [52], Jaya algorithm [53], [54], and teaching-learning based optimization (TLBO) [55], [56] are some of the algorithms implemented to tune PID controllers for AGC.

In this paper, rank exponent (RE) method-based proportional-integral-derivative controller with derivative filtering (PIDm) is designed for AGC problem of two-area power systems. ITAE of tie-line power deviations, ITAE of ACEs, and frequency deviations in area 1 and area 2 are considered as sub-objectives while designing the overall objective for tuning the PIDm controller. This overall objective function is the weighted sum of the three sub-objectives considered. In this article, RE method is used to determine the weights corresponding to sub-objectives. The RE method takes care of the relative significance of sub-objectives while obtaining the weights. This helps in designing more appropriate objective function for tuning of controller parameters. The overall objective function is minimized using Jaya algorithm. Comparative analysis is

performed for Jaya-based controller along with salp swarm algorithm (SSA), symbiotic organisms search (SOS), Nelder-Mead simplex (NMS), elephant herding optimization (EHO), and Luus-Jaakola (LJ) algorithms-based controllers to prove efficacy and effectiveness of the proposed controller. Six test cases with various load fluctuations are examined in this study to confirm the findings of the work. Moreover, non-parametric test and statistical analysis are also performed to prove the applicability of RE method in designing the Jaya-based controller. The Friedman rank test as no-parametric statistical analysis is provided in the determination of significance level of presented optimization algorithms whereas statistical measures are evaluated with the help of statistical analysis. The prime contributions of the presented work are highlighted as follows:

- PIDm controller is designed to deal with optimal control of AGC for two-area interconnected power systems.
- For better control strategy, ITAE of tie-line power deviations, ITAE of ACEs, and frequency deviation in area 1 and area 2 are considered to frame objective function.
- The weighted objective function is formulated by incorporating the RE method to assign the weights associated with each sub-objectives.
- The minimization of resultant objective function is done with the help of Jaya algorithm.
- Further, the efficacy and applicability of the presented Jaya assisted control design approach is proved by Friedman rank test and statistical analysis in comparison to other algorithms such as SSA, SOS, NMS, EHO, and LJ optimization algorithms.

The structure of this paper is as follows: Section II briefly introduces both the power system and PIDm controller. Constraints of controller and problem formulation are discussed in Section III. Section IV demonstrates RE method and its implementation in AGC. Jaya algorithm is given in Section V. Simulated results are briefly discussed in Section VI. Conclusion is demonstrated in Section VII.

II. POWER SYSTEM

An electric power system consists of electrical components that are utilized for generation, transmission, and distribution of power. Electric power is produced by a large number of linked generators to meet the load requirement. These generators are interlinked with transmission lines to transfer the power from generating end to consumer end, at rated frequency and voltage. Generally, different types of resources are utilized for generation of electric power. These resources are mainly categorized into conventional and non-conventional resources. Coal, gas, nuclear and hydro-generations are the main conventional resources for the generation of electrical energy. However, biomass, solar, wind, tidal, wave, etc. are various sources of non-conventional resources for the generation of electricity. These sources initially transform the produced energy into mechanical energy. Then, with the help of generators, electrical energy is obtained from this mechanical energy. Generated electrical energy is transmitted via overhead transmission lines to distribution substations. The distribution of power to commercial, residential, and industrial consumers is managed by distribution substations.

The demand for power increases along with an increase in load. To meet the increasing demand, additional power is to be extracted from the generator. In a single-area power system, increased load demand is fed by increasing generation or borrowing kinetic energy from interconnected machines. While in a multi-area system, power supply from interconnected generators through tie-lines is used which helps in supplying power to load from interconnected generating units. Due to borrowing power from interconnected area, the stress on generating units of area, in which load demand is increased, decreases.

A. POWER SYSTEM MODEL UNDER INVESTIGATION

Model of a two-area interconnected power system investigated in this work is shown in Fig. 1. The two-area interconnected power system is considered and its specifications are taken from Ali and Abd-Elazim [57]. Two thermal power plants with 2000 MW combined capacity and 1000 MW load of each plant, make up the realistically linked system. Fig. 1 shows a network of two-area power system, where Δf_{r1} and Δf_{r2} are variations in system frequencies. Area control errors are ACE_{r1} and ACE_{r2}; frequency bias factors are β_{r1} and β_{r2}; and control inputs are μ_{r1} and μ_{r2}, respectively. Governors' speed regulation constants are R_{r1} and R_{r2}, time constants of governors are T_{g1} and T_{g2} and time constants of turbines are T_{t1} and T_{t2}, respectively. G_{r1} and G_{r2} are gains of both areas. Power system time constants are T_{r1} and T_{r2}. Governor power deviations are ΔP_{g1} and ΔP_{g2}. Non-reheat steam turbine power deviations are ΔP_{t1} and ΔP_{t2}, and variations in load requirements of power system in areas 1 and 2 are ΔP_{lr1} and ΔP_{lr2}, respectively. Interconnected power system's tie-line power variation is indicated by ΔP_{tl}.

B. PIDM CONTROLLER'S CONFIGURATION

PID controller is broadly preferred in industrial control applications [58]. The reasons are; (i) easier understanding, (ii) easier tuning, and (iii) easier implementation. In this contribution, the adopted structure of PID controller [59] is shown in Fig. 2. PID control scheme consists of three controlling terms, which form the manipulated variable (MV). These three controlling terms are proportional, integral, and derivative gains. These are represented by ϕ_p, ϕ_i, and ϕ_d, respectively. The output of the controller is given as follows

$$u(t) = \phi_p.e(t) + \phi_i \int_0^t e(t).dt + \phi_d \frac{\mathrm{d}}{\mathrm{dt}} e(t) \qquad (1)$$

where, $u(t)$ describes PID controller's output and $e(t)$ denotes the error signal.

To obtain optimum response, the controlling parameters need to be tuned. The detrimental effect of noise in signal's input is mitigated by using a filter and a derivative gain.

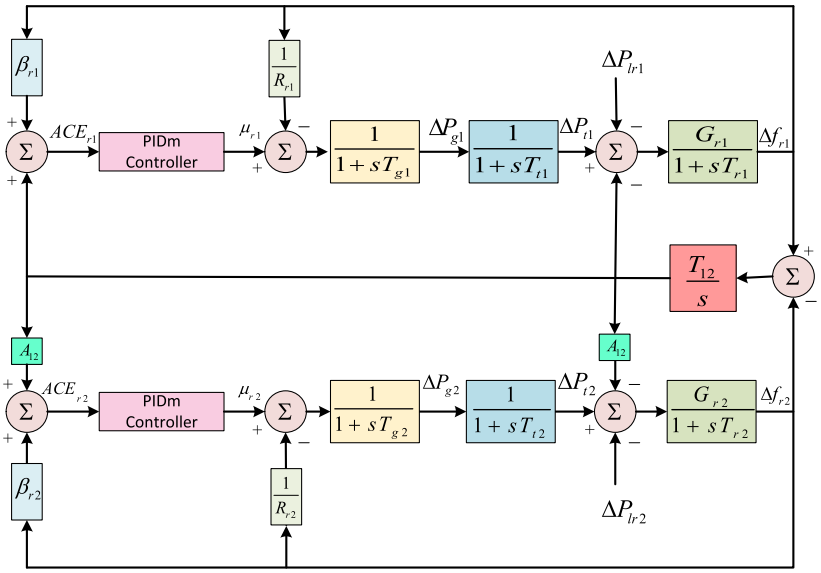

FIGURE 1. Interconnected power system of two-area.

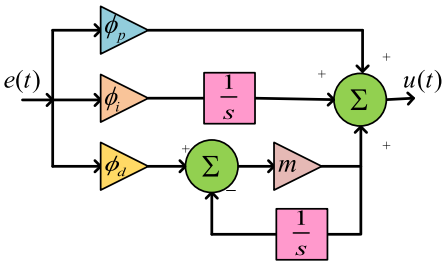

FIGURE 2. Configuration of controller.

The frequency domain response of the PID controller with derivative filter (commonly known as PIDm controller) is written as follows:

$$TF_{PIDm} = \phi_p + \phi_i\left(\frac{1}{s}\right) + \phi_d\left(\frac{1}{\frac{1}{m}+\frac{1}{s}}\right) \tag{2}$$

where, m is the filter coefficient. Area control errors, ACE_{r1} and ACE_{r2} of areas 1 and 2 respectively, act as inputs to controllers. The expressions for ACE_{r1} and ACE_{r2} are provided in (3) and (4).

$$ACE_{r1}(s) = \Delta P_{tl12}(s) + \beta_{r1} \cdot \Delta f_{r1}(s) \tag{3}$$

$$ACE_{r2}(s) = A_{12} \cdot \Delta P_{tl12}(s) + \beta_{r2} \cdot \Delta f_{r2}(s) \tag{4}$$

The parameter A_{12} is taken as (-1).

III. PROBLEM FORMULATION

The major factors that are affected by sudden changes in load are voltage and frequency of generator. A consistent increment in load demand and merging of renewable power sources with existing power systems, increase the complexity of system. As the complexity of system increases, maintaining reliability and continuity of power supply, and achieving stable operation becomes challenging. To overcome these issues, AGC is used. AGC aims to reduce frequency fluctuations while meeting system limits to maximize consistent and dependable power flow in MA linked power system. For stable operation, the parameters of PIDm controller demonstrated in Fig. 2 needs to be tuned within a specific range of parameter variations. The formulation of an objective function is necessary to figure out the best possible solution to this issue.

A. FORMULATION OF OBJECTIVE FUNCTION

The deviations in tie line power, voltage, and frequency are controlled by controller, based on error function. For formulation of objective function, integral time absolute error (ITAE), integration of squared error (ISE) [22], integral of time multiplied square error (ITSE), or integration of absolute error (IAE) may be considered. ITAE is taken into consideration for minimization of area control errors, deviations in tie-line power, and frequency deviations in generators, in this work. The objectives that are minimized, are given as:.

$$\varphi_1 = \int_0^{\tau_s} \|\Delta f_{r1}\| t\, dt + \int_0^{\tau_s} \|\Delta f_{r2}\| t\, dt \tag{5}$$

$$\varphi_2 = \int_0^{\tau_s} \|\Delta P_{tl}\| t\, dt \tag{6}$$

$$\varphi_3 = \int_0^{\tau_s} \|ACE_{r1}\| t\, dt + \int_0^{\tau_s} \|ACE_{r2}\| t\, dt \tag{7}$$

In (5), (6) and (7), total simulation time is denoted by τ_s. While, φ_1, φ_2, and φ_3 are objective functions. The combined effect of ITAEs with variations in frequency of areas 1 and 2 are represented by φ_1. While, φ_2 denotes the ITAEs of

fluctuations in tie-line power. ITAEs of area control errors in both areas are signified by φ_3. Overall objective function is formulated by considering (5), (6) and (7), as:

$$\varphi(\varphi_1, \varphi_2, \varphi_3) = \delta_1\varphi_1 + \delta_2\varphi_2 + \delta_3\varphi_3 \tag{8}$$

where, weights of objectives φ_1, φ_2, and φ_3 are δ_1, δ_2, and δ_3, respectively. The significance of φ_1, φ_2, and φ_3 in φ is given by these weights. By obtaining the values of φ_1, φ_2, and φ_3 from (5), (6), and (7) and utilizing them for (8), (9) is obtained.

$$\left.\begin{aligned}\varphi = \delta_1\left(\int_0^{\tau_s}\|\Delta f_{r1}\|t\ dt + \int_0^{\tau_s}\|\Delta f_{r2}\|t\ dt\right)\\ +\delta_2\int_0^{\tau_s}\|\Delta P_{tl}\|t\ dt\\ +\delta_3\left(\int_0^{\tau_s}\|ACE_{r1}\|t\ dt + \int_0^{\tau_s}\|ACE_{r2}\|t\ dt\right)\end{aligned}\right\} \tag{9}$$

In this article, weights δ_1, δ_2, and δ_3 related with (9) are determined by using the rank exponent (RE) method [60] which is further discussed in section IV.

B. CONSTRAINTS OF PIDM CONTROLLER

Constraints play a significant role in decision-making whenever load disturbances occur in any area. Parameters of controller, i.e. ϕ_p, ϕ_i, ϕ_d, and m, are decision variables as represented in Fig. 2. Controllers have limitations in varying the range of controller parameters. The following boundary constraints are taken into consideration for controller parameters:

$$\phi_p^{min} < \phi_p < \phi_p^{max} \tag{10}$$
$$\phi_i^{min} < \phi_i < \phi_i^{max} \tag{11}$$
$$\phi_d^{min} < \phi_d < \phi_d^{max} \tag{12}$$
$$m^{min} < m < m^{max} \tag{13}$$

IV. METHODOLOGY

A. RANK EXPONENT METHOD

In AGC, stability and reliability of an electrical power system depends on maintaining a balance between generation and load demand. To achieve this, different control objectives, such as frequency regulation, tie-line power control, and economic dispatch, need to be prioritized. In the context of multi-criteria evaluation, it is important to recognize that the sub-objectives contributing to overall objective are not of equal significance. Therefore, to enhance decision-making accuracy, it is essential to assign weights to these objectives. In literature [28], [60], [61], [62], a variety of weighting methods are suggested to assign weights. These techniques include equal weighting, rank exponent (RE), rank reciprocal, rank of centroid, and rank-sum method. RE method stands out among these weight estimation techniques due to incorporation of weight distribution factor. By appropriately selecting distribution factor value, it becomes possible to modulate the distribution of weights among the available

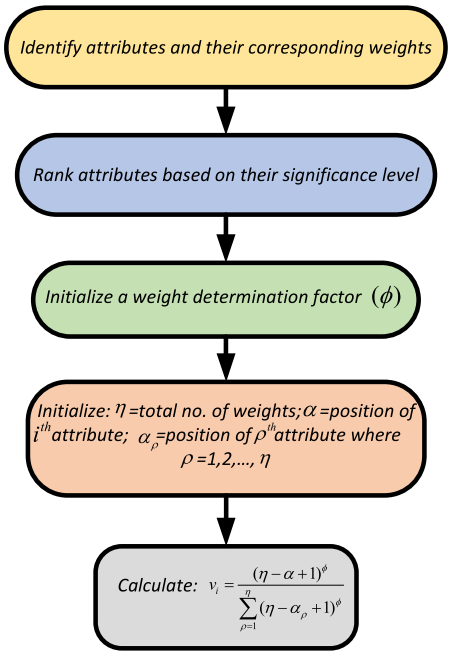

FIGURE 3. Stepwise implementation of RE method.

options, making it a preferred choice. Rank exponent weight method is an extension of rank-sum weight method [28]. The formula for determining the weights is represented as:

$$v_i = \frac{(\eta - \alpha + 1)^{\varnothing}}{\sum_{\rho=1}^{\eta}\left(\eta - \alpha_\rho + 1\right)^{\varnothing}} \tag{14}$$

In (14), total number of attributes are denoted by η while α indicates attribute's position. Normalized weights of α^{th} attribute are given by v_i. Weight distribution parameter $\varnothing$, distributes the weights in a stepper way as its value inclines.

B. IMPLEMENTATION OF RE IN AGC

Implementation of RE method for AGC problem is shown in Fig. 3. For implementation, sub-objectives φ_1, φ_2, and φ_3 are considered as attributes ($\eta = 3$). The value of weight determination factor $\varnothing$ is considered to be 3 in order to illustrate the distribution of weights in an exponential way. Ranking of attributes is given in Table 1.

TABLE 1. Attributes' ranking.

ine	Attribute	Rank position (α)
ine	φ_1	1
	φ_2	2
	φ_3	3
ine		

Ranking order of attributes is considered as φ_1, φ_2, and φ_3 in sequence. Normalized weights of each objectives

are obtained using (14) as follows:

$$\left.\begin{aligned}\delta_1 &= 0.75\\ \delta_2 &= 0.2222\\ \delta_3 &= 0.0277\end{aligned}\right\} \tag{15}$$

Eq. (15) shows significance of every objective in overall objective function. Thus, complete objective function (8) with φ_1, φ_2, and φ_3 and their weights δ_1, δ_2, and δ_3, respectively, turns out to be

$$\varphi(\varphi_1, \varphi_2, \varphi_3) = 0.75\,\varphi_1 + \ 0.2222\,\varphi_2 + \ 0.0277\,\varphi_3\} \tag{16}$$

However, overall objective function (9) changes to

$$\left.\begin{aligned}\varphi = 0.75&\left(\int_0^{\tau_s} \|\Delta f_{r1}\| t\ dt + \int_0^{\tau_s} \|\Delta f_{r2}\| t\ dt\right)\\ &+0.2222 \int_0^{\tau_s} \|\Delta P_{tl}\| t\ dt\\ &+0.0277\left(\int_0^{\tau_s} \|ACE_{r1}\| t\ dt + \int_0^{\tau_s} \|ACE_{r2}\| t\ dt\right)\end{aligned}\right\} \tag{17}$$

In (17), three sub-objectives are presented with their associated weights. Since, the higher priority is assigned to improvement on frequency deviations in area 1 and area 2, the higher weight i.e. 0.75 is considered for the first sub-objective. Further, the second priority is considered for improvement on ITAE of tie-line power deviations. Thus, the weight of 0.2222 is assigned to it. Furthermore, the last priority is improvement on ITAE of ACEs in area 1 and area 2. So, the least weight i.e. 0.0277 is assigned for the sub-objective of ITAE of ACEs in area 1 and area 2. This systematic allotment of weights for each sub-objective helps to improve the weighted objective function in attaining the suitable AGC for an interconnected power system. The obtained weighted objective function given in (17) is minimized using Jaya optimization algorithm, subject to constraints specified in (10), (11), (12), and (13).

V. JAYA OPTIMIZATION ALGORITHM

In Sanskrit, term ''Jaya'' is synonymous with victory. This semantic correspondence serves as primary motivational driving force for Jaya algorithm to approach success and evade failure. Jaya algorithm is characterized as a parameter-free, population-based metaheuristic optimization technique, initially proposed by Rao [63]. This algorithm exclusively depends on conventional control parameters (specifically population size and number of iterations for optimization [64]). Its scope extends to address both, unconstrained and constrained optimization problems. The algorithm draws inspiration from natural concept of survival of fittest. Candidate solutions in this approach gravitate towards global best solution while avoiding worst solution. This algorithm identifies worst and best solutions among the candidate solutions and subsequently updates each solution by converging towards best solution and diverging from worst solution.

Jaya algorithm: Pseudocode

Set parameters N, L and M.
  i=1
  while (i<N) do
    Determine $f(\xi_{\mu,l})$
    Find $f(\xi_{best,l})$ and $f(\xi_{worst,l})$
      for μ =1 to M, ***do***
        for l =1 to L, ***do***
          Obtain $Z_1 \in [0,1]$ and $Z_2 \in [0,1]$
          Calculate $X_1 = Z_1[\xi_{best,l} - \xi_{\mu,l}]$; $X_0 = -Z_2[\xi_{worst,l} - \xi_{\mu,l}]$
          Compute $\xi'_{\mu,l} = \xi_{\mu,l} + X_1 + X_0$
        End for
        if $f(\xi'_i) < f(\xi_i)$ ***then***
          $\xi_i \leftarrow \xi'_i$
        End if
      End for
      $i \leftarrow i+1$
  End while

FIGURE 4. Pseudocode of Jaya algorithm.

Let M be the number of candidate solutions (i.e. population size, μ=1,2,$\cdots$,M), updated variables of each solution at i^{th} iteration for l^{th} design variable (i.e. l=1,2,$\cdots$,L) is given by,

$$\xi'_{\mu,l} = \xi_{\mu,l} + X_1 + X_0 \tag{18}$$

where,

$$X_1 = Z_1 \times \left(\xi_{best,l} - \xi_{\mu,l}\right) \tag{19}$$

$$X_0 = -Z_2 \times \left(\xi_{worst,l} - \xi_{\mu,l}\right) \tag{20}$$

In (18), $\xi_{\mu,l}$ represents current candidate solution and $\xi'_{\mu,l}$ indicates updated candidate solution. In (19) and (20), $\xi_{best,l}$ denotes best candidate solution, $\xi_{worst,l}$ signifies worst candidate solution, while Z_1 and Z_2 are random parameters ranging from zero to unity. The terms X_1 and X_0 indicate a solution's tendency to get closer to optimal solution and avoid worst solution, respectively. Updated candidate solution is acceptable only if it is better than existing candidate solution. After completion of every iteration, selected candidate solutions act as input for successive iteration procedure. Fig. 4 shows Jaya algorithm's pseudocode where N denotes total iterations. This algorithm constantly aims to minimize failure (i.e., moving away from worst candidate solution) and to increase its probability to succeed (i.e., locate the best candidate solution).

VI. RESULTS AND DISCUSSION

In this paper, interconnected two-area power system is investigated, as described in Ali and Abd-Elazim [57]. Constraints of controller parameters are defined in (10), (11),

TABLE 2. Case studies.

ine	Step load variations	
Test cases	Area 1	Area 2
ine ine 1	0.04	0
ine 2	0	0.04
ine 3	0.04	0.04
ine 4	0.04	-0.04
ine 5	0.04	0.08
ine 6	0.08	0.04
ine		

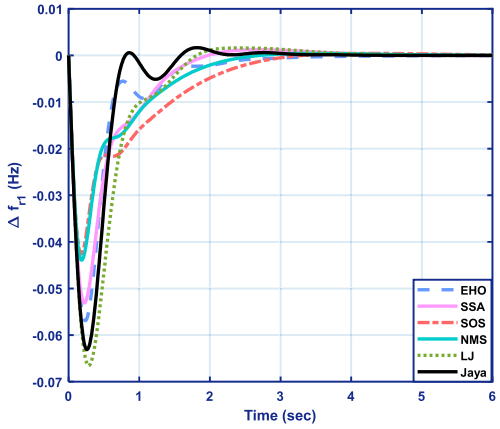

FIGURE 5. Δf_{r1} for Case 1.

(12), and (13). However, overall objective function to be minimized in shown in (17). The boundary conditions for controller parameters, defined in (10), (11), (12), and (13), are provided in Appendix A. While, the system parameters taken from [57] are tabulated in Appendix B. To effectively evaluate the performance of RE method-assisted PIDm controller, six test cases are considered that are tabulated in Table 2. This table provides the step load disturbance given to each area in all six cases. The test results of different cases (Cases 1-6) are tabulated in Tables 3-8. The performance of PIDm controller with different algorithms (Nelder-Mead simplex (NMS), elephant herding optimization (EHO) [65], symbiotic organisms search (SOS), salp swarm algorithm (SSA), and Luus-Jaakola (LJ) [66] algorithm) are compared with Jaya-based PID controller in these tables. Also, values of controller parameters, ϕ_p, ϕ_i, ϕ_d, and m corresponding to minimum value of objective function, are provided in these tables. Moreover, minimum value of fitness function, corresponding value of settling time and overshoot are tabulated in Tables 3-8.

Performance analysis for controllers, designed with Jaya, SOS, EHO, SSA, LJ, and NMS algorithms, is also performed. Each optimization algorithm is run 50 times, with 50 iterations, for each of six test cases stated above. Total of hundred solutions are investigated for each algorithm. Jaya, SSA, EHO, SOS, NMS, and LJ algorithms' parameters are utilized for this work are listed in Appendix C. Table 9 represents the results of this comparison analysis. Test results of Case 1 are tabulated in Table 3. Fig(s). 5, 6, and 7 illustrate the variations in frequencies (Δf_{r1} and Δf_{r2}) of areas 1 and 2,

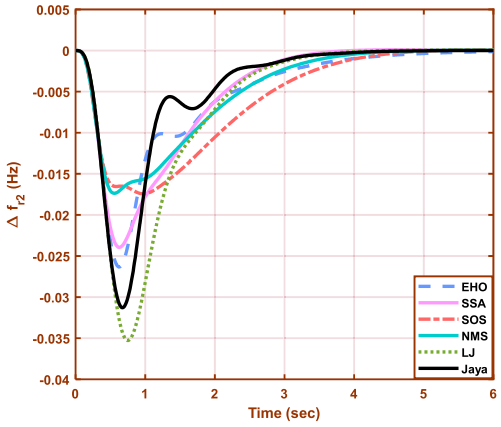

FIGURE 6. Δf_{r2} for Case 1.

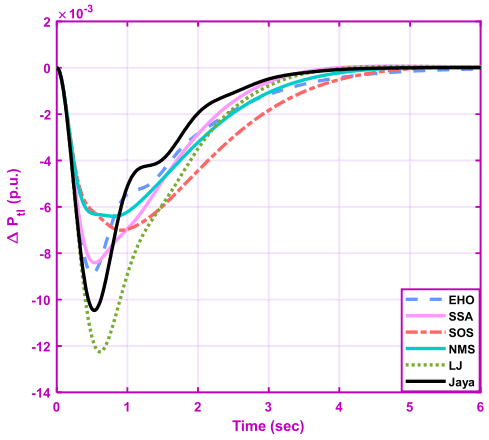

FIGURE 7. ΔP_{tl} for Case 1.

and variation in tie-line power (ΔP_{tl}), respectively, under Case 1. The values of sub-objectives, φ_1, φ_2, and φ_3 should be low for optimal solution of overall objective function shown in (9). Jaya-based PIDm controller gives best optimal values of sub-objectives as compared to others. Table 3 exemplifies that Jaya-based PIDm controller achieves quickest settling times for tie-line power, as well as frequency deviations in both areas.

Table 4 provides the outcomes of Case 2. The recommended Jaya-based PIDm controller accomplishes least value of φ under loading conditions described in Case 2. The frequency fluctuations of area-1, area-2, and tie-line power deviation are shown in Fig(s). 8, 9, and 10, respectively. The simulation results show that Jaya-based PIDm controller offers least settling time for power flow variations along the tie-line power deviation which shows Jaya-based controller outperforms the other five. For Case 3, frequency fluctuations in area-1, area-2, and tie-line power variation are presented in Fig(s). 11, 12, and 13. In Case 3, there is an equal load deviation in both areas. Consequently, tie-line power deviation is reduced to zero, as illustrated in Fig. 13. The outcomes of Case 3 are comprehensively tabulated in Table 5. Frequency fluctuations in both areas have achieved shortest

TABLE 3. Test results of case 1.

ine		EHO	SSA	SOS	NMS	LJ	Jaya
ine	φ	0.0528	0.0478	0.0752	0.0514	0.0595	**0.0360**
Fitness	φ_1	0.0638	0.0582	0.0915	0.0624	0.0724	**0.0435**
	φ_2	0.0187	0.0157	0.0246	0.0173	0.0196	**0.0127**
	φ_3	0.0290	0.0236	0.0387	0.0261	0.0302	**0.0192**
ine	ϕ_p	2.6885	2.1105	2.4265	2.7621	1.4022	2.1822
Controller parameters	ϕ_i	2.6337	2.7594	2.2941	2.8268	2.1428	2.9884
	ϕ_d	0.7650	0.9683	1.4862	1.3483	0.6165	0.6241
	m	420.93	180.87	204.02	421.63	385.57	305.17
ine	Δf_{r1}	2.3712	3.1068	2.8498	2.3004	2.9826	**1.9583**
Settling time (s)	Δf_{r2}	4.6258	3.3413	4.5532	4.1181	3.3378	**3.3204**
	ΔP_{tl}	4.8315	3.5240	4.6616	4.2402	3.5214	**3.5147**
ine	Δf_{r1}	0.0569	0.0531	0.0426	0.0439	0.0666	0.0631
Maximum overshoots (p.u.)	Δf_{r2}	0.0263	0.0240	0.0174	0.0174	0.0353	0.0313
	ΔP_{tl}	0.0089	0.0084	0.0070	0.0064	0.0123	0.0105
ine							

TABLE 4. Test results of case 2.

ine		EHO	SSA	SOS	NMS	LJ	Jaya
ine	φ	0.0567	0.0540	0.0512	0.0516	0.0503	**0.0359**
Fitness	φ_1	0.0699	0.0665	0.0622	0.0625	0.0612	**0.0438**
	φ_2	0.0157	0.0154	0.0172	0.0178	0.0168	**0.0116**
	φ_3	0.0277	0.0262	0.0263	0.0280	0.0259	**0.0183**
ine	ϕ_p	1.4920	1.7913	1.5621	1.5136	1.5267	1.8637
Controller parameters	ϕ_i	2.7745	2.9361	2.3342	2.2527	2.3451	2.9993
	ϕ_d	0.8456	1.0252	0.5897	0.5047	0.5625	0.5519
	m	305.00	423.19	436.65	402.54	438.07	433.24
ine	Δf_{r1}	3.9316	4.2446	3.3750	3.5153	3.3387	**3.1572**
Settling time (s)	Δf_{r2}	3.4775	3.6343	2.3046	2.2658	2.3771	**2.2451**
	ΔP_{tl}	4.4595	4.7093	3.4971	3.5842	3.4298	**3.0981**
ine	Δf_{r1}	0.0283	0.0237	0.0352	0.0386	0.0363	0.0347
Maximum overshoots (p.u.)	Δf_{r2}	0.0577	0.0518	0.0669	0.0712	0.0683	0.0671
	ΔP_{tl}	0.0101	0.0085	0.0121	0.0131	0.0124	0.0116
ine							

TABLE 5. Test results of case 3.

ine		EHO	SSA	SOS	NMS	LJ	Jaya
ine	φ	0.0975	0.0959	0.0707	0.0745	0.0814	**0.0445**
Fitness	φ_1	0.1280	0.1259	0.0929	0.0978	0.1068	**0.0585**
	φ_2	0	0	0	0	0	0
	φ_3	0.0544	0.0535	0.0395	0.0415	0.0454	**0.0248**
ine	ϕ_p	2.0917	1.3972	1.7582	1.8066	1.8639	1.7031
Controller parameters	ϕ_i	2.3741	2.7126	2.7016	2.5997	2.5488	2.9905
	ϕ_d	0.6839	0.7993	0.7664	0.7807	0.8541	0.5389
	m	335.26	226.47	299.01	311.96	291.81	240.14
ine	Δf_{r1}	3.5070	3.6976	2.1884	2.3966	2.5621	**1.6024**
Settling time (s)	Δf_{r2}	3.5070	3.6976	2.1884	2.3966	2.5621	**1.6024**
	ΔP_{tl}	0	0	0	0	0	0
ine	Δf_{r1}	0.0685	0.0673	0.0667	0.0659	0.0629	0.0776
Maximum overshoots (p.u.)	Δf_{r2}	0.0685	0.0673	0.0667	0.0659	0.0629	0.0776
	ΔP_{tl}	0	0	0	0	0	0
ine							

settling time using Jaya-based PIDm controller. The overall objective function, φ, and sub-objectives, φ_1, φ_2, and φ_3, are obtained minimum in case of recommended Jaya-based PIDm controller.

Similarly, Table 6 presents results of Case 4. The data presented in Table 6 highlights that Jaya-based controller attains the minimum value for φ, along with its objectives φ_1, φ_2, and φ_3. The frequency variations in area-1, area-2, and tie-line power variation are depicted in Fig(s). 14, 15, and 16, respectively. These figures demonstrate that PIDm controller based on Jaya performs better than others.

Test results of Case 5 are presented in Table 7. The values of φ, φ_1, φ_2, and φ_3 are observed as least after implementing recommended Jaya-based PIDm controller. Fig. 17, Fig. 18, and Fig. 19 depict frequency fluctuations observed in areas 1 and 2, as well as tie-line power variation, respectively. The recommended Jaya-based PIDm controller has smallest settling time for frequency fluctuations in areas 1 and 2, and tie-line power deviation.

TABLE 6. Test results of case 4.

ine		EHO	SSA	SOS	NMS	LJ	Jaya
ine	φ	0.0669	0.0669	0.0607	0.0592	0.0594	**0.0586**
Fitness	φ_1	0.0706	0.0726	0.0673	0.0687	0.0681	**0.0655**
	φ_2	0.0526	0.0473	0.0392	0.0297	0.0392	**0.0290**
	φ_3	0.0818	0.0711	0.0571	0.0412	0.0566	**0.0401**
ine	ϕ_p	2.7806	2.2702	2.6629	1.7886	2.4937	1.7964
Controller parameters	ϕ_i	2.2974	2.2744	2.5671	2.7919	2.5077	2.8286
	ϕ_d	1.7427	1.3041	0.6756	0.8600	0.8860	0.8549
	m	243.07	431.27	406.99	162.39	472.92	159.82
ine	Δf_{r1}	4.8159	4.3453	3.7214	3.2865	3.8597	**3.2609**
Settling time (s)	Δf_{r2}	4.8159	4.3453	3.7214	3.2865	3.8597	**3.2609**
	ΔP_{tl}	5.2087	4.5151	4.9439	3.0721	4.7178	**3.0411**
ine	Δf_{r1}	0.0371	0.0426	0.0554	0.0528	0.0502	0.0529
Maximum overshoots (p.u.)	Δf_{r2}	0.0371	0.0426	0.0554	0.0528	0.0502	0.0529
	ΔP_{tl}	0.0128	0.0147	0.0190	0.0189	0.0169	0.0189
ine							

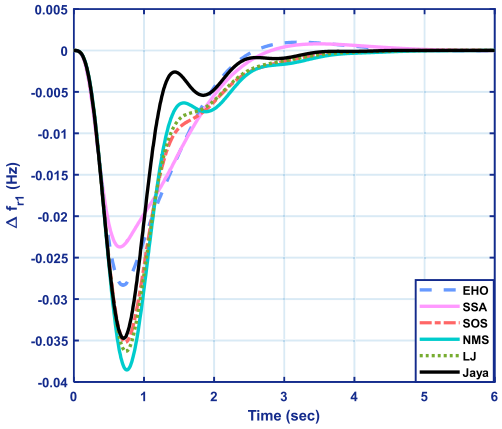

FIGURE 8. Δf_{r1} for case 2.

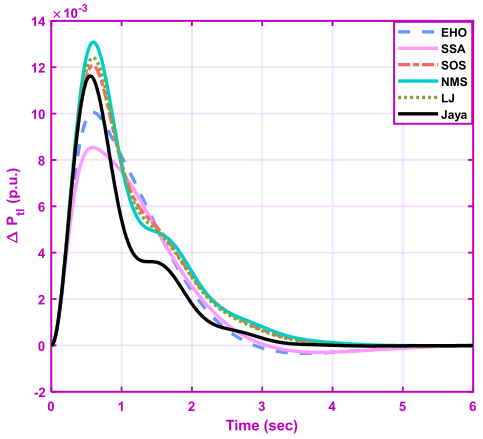

FIGURE 10. ΔP_{tl} for case 2.

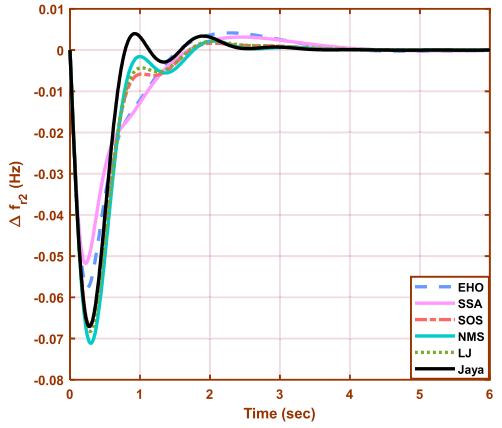

FIGURE 9. Δf_{r2} for case 2.

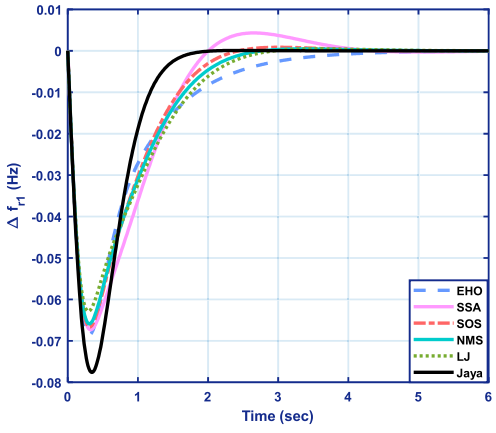

FIGURE 11. Δf_{r1} for case 3.

Similarly, test results of Case 6 are tabulated in Table 8. Frequency fluctuations of area-1, area-2, and tie-line power deviation produced by the suggested Jaya-based PIDm controller for the loading condition stated in Case 6 are shown in Fig. 20, Fig. 21 and Fig. 22, respectively. According to this data, recommended Jaya-based PIDm controller provides the least settling time for variations in frequency of both regions and tie-line power deviation. Because of this, the recommended Jaya-based PIDm controller precisely outperforms other controllers for Case 6 also.

A statistical evaluation is conducted to analyze the efficacy of recommended Jaya-based PIDm controller. In Table 9, the lowest, average, highest, and standard deviation values of each case are tabulated. The recommended Jaya-based

TABLE 7. Test results of case 5.

ine		EHO	SSA	SOS	NMS	LJ	Jaya
ine	φ	0.1562	0.1083	0.2063	0.1782	0.2264	**0.0763**
Fitness	φ_1	0.1997	0.1377	0.2633	0.2275	0.2892	**0.0968**
	φ_2	0.0187	0.0150	0.0261	0.0218	0.0273	**0.0112**
	φ_3	0.0841	0.0627	0.1108	0.0960	0.1224	**0.0420**
ine	ϕ_p	2.6975	1.6974	1.2583	2.2825	2.0957	1.6745
Controller parameters	ϕ_i	2.8269	2.5587	1.8311	2.4080	2.0554	2.9679
	ϕ_d	1.6113	0.3824	0.7105	1.3164	1.2755	0.4826
	m	375.93	482.04	438.73	437.26	413.27	414.86
ine	Δf_{r1}	3.5213	3.4694	3.1653	3.7133	4.2221	**2.3926**
Settling time (s)	Δf_{r2}	2.9397	2.8027	2.5675	3.0758	3.5427	**2.1385**
	ΔP_{tl}	4.0098	3.3440	3.8163	4.2355	4.7317	**3.0782**
ine	Δf_{r1}	0.0498	0.1064	0.0953	0.0587	0.0623	0.0986
Maximum overshoots (p.u.)	Δf_{r2}	0.0828	0.1622	0.1345	0.0933	0.0955	0.1508
	ΔP_{tl}	0.0063	0.0139	0.0119	0.0073	0.0078	0.0127
ine							

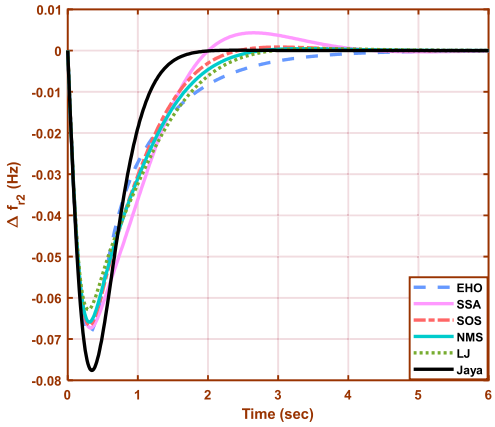

FIGURE 12. Δf_{r2} for case 3.

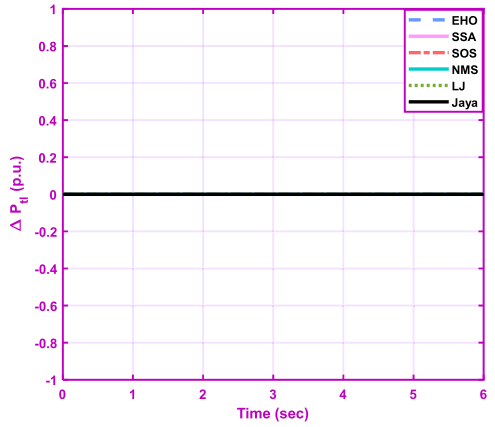

FIGURE 13. ΔP_{tl} for case 3.

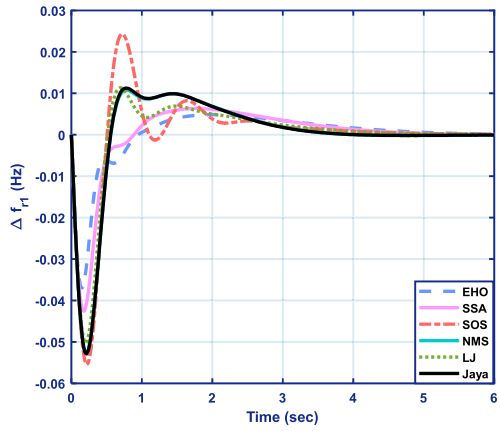

FIGURE 14. Δf_{r1} for case 4.

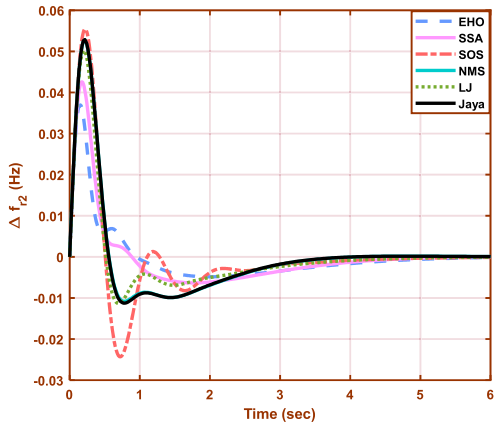

FIGURE 15. Δf_{r2} for case 4.

PIDm controller provides the best value in every scenario, as this table demonstrates. The next best choice is an SOS-based controller, which is followed by an NMS-based controller. The recommended Jaya-based PIDm controller provides the least values for lowest, average, highest, and standard deviation for objective function. This statistical study demonstrates that recommended Jaya-based PIDm controller performs superior to other controllers tuned using NMS, SSA, EHO, SOS, and LJ algorithms.

Friedman rank test [67], a non-parametric statistical test, is also used to evaluate the significance of outcomes obtained with suggested controller. The null hypothesis assumes that the outcomes of other algorithms are not significantly

TABLE 8. Test results of case 6.

ine		EHO	SSA	SOS	NMS	LJ	Jaya
ine	φ	0.0789	0.0891	0.0854	0.2292	0.1581	**0.0776**
Fitness	φ_1	0.1002	0.1133	0.1085	0.2931	0.2017	**0.0985**
	φ_2	0.0117	0.0130	0.0123	0.0267	0.0200	**0.0115**
	φ_3	0.0417	0.0461	0.0462	0.1245	0.0856	**0.0412**
ine	ϕ_p	1.8091	1.7268	2.1149	2.9995	2.4728	1.7876
Controller parameters	ϕ_i	2.9558	2.7829	2.9997	2.2853	2.4975	2.9768
	ϕ_d	0.5324	0.5653	0.5247	0.4459	1.1471	0.5249
	m	288.75	373.52	446.97	487.34	329.87	403.92
ine	Δf_{r1}	1.6081	1.6614	2.4000	4.4673	3.1881	**1.5836**
Settling time (s)	Δf_{r2}	2.4149	2.4639	3.1490	5.8026	4.0251	**2.3932**
	ΔP_{tl}	3.1003	3.1427	3.2923	5.8179	4.5271	**3.0813**
ine	Δf_{r1}	0.1444	0.1421	0.1417	0.1409	0.0999	0.1451
Maximum overshoots (p.u.)	Δf_{r2}	0.0934	0.0929	0.0899	0.0861	0.0607	0.0942
	ΔP_{tl}	0.0119	0.0118	0.0114	0.0108	0.0073	0.0120
ine							

TABLE 9. Statistical analysis.

ine **Cases**	**Statistical measures**	**EHO**	**SSA**	**SOS**	**NMS**	**LJ**	**Jaya**
ine	Lowest	0.0528	0.0478	0.0752	0.0514	0.0595	**0.0360**
I	Average	0.0760	0.0678	0.0787	0.0717	0.0721	**0.0365**
	Highest	0.1147	0.0874	0.0826	0.0856	0.0810	**0.0373**
	Standard deviation	0.0258	0.0191	0.0033	0.0125	0.0096	**0.0006**
ine	Lowest	0.0567	0.0540	0.0512	0.0516	0.0503	**0.0359**
II	Average	0.0873	0.1417	0.0536	0.0560	0.0574	**0.0389**
	Highest	0.1312	0.3611	0.0569	0.0592	0.0624	**0.0455**
	Standard deviation	0.0274	0.1258	0.0040	0.0032	0.0047	**0.0028**
ine	Lowest	0.0975	0.0959	0.0707	0.0745	0.0814	**0.0445**
III	Average	0.1489	0.1316	0.0842	0.0895	0.0867	**0.0470**
	Highest	0.2623	0.1902	0.1071	0.1062	0.0923	**0.0525**
	Standard deviation	0.0662	0.0353	0.0136	0.0148	0.0051	**0.0032**
ine	Lowest	0.0669	0.0669	0.0607	0.0592	0.0594	**0.0586**
IV	Average	0.0884	0.0698	0.0742	0.0623	0.0998	**0.0611**
	Highest	0.1142	0.0734	0.1008	0.0652	0.1460	**0.0646**
	Standard deviation	0.0199	0.0028	0.0161	0.0024	0.0369	**0.0022**
ine	Lowest	0.1562	0.1083	0.2063	0.1782	0.2264	**0.0763**
V	Average	0.2334	0.1964	0.2232	0.2135	0.2307	**0.0800**
	Highest	0.3560	0.2712	0.2289	0.2437	0.2347	**0.0859**
	Standard deviation	0.0865	0.0616	0.0096	0.0288	0.0038	**0.0037**
ine	Lowest	0.0789	0.0891	0.0854	0.2292	0.1581	**0.0776**
VI	Average	0.0896	0.2381	0.1601	0.2867	0.1633	**0.0864**
	Highest	0.1080	0.4389	0.2684	0.3887	0.1748	**0.1008**
	Standard deviation	0.0094	0.1744	0.0746	0.0659	0.0133	**0.0068**
ine							

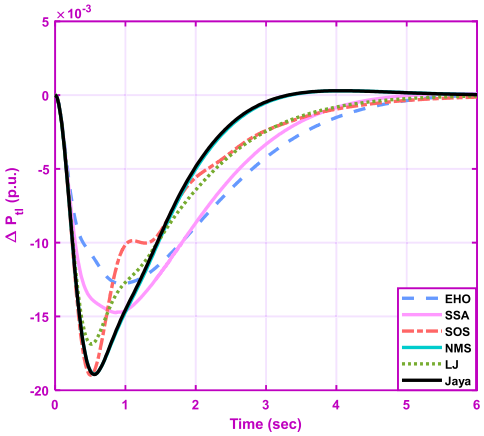

FIGURE 16. ΔP_{tl} for case 4.

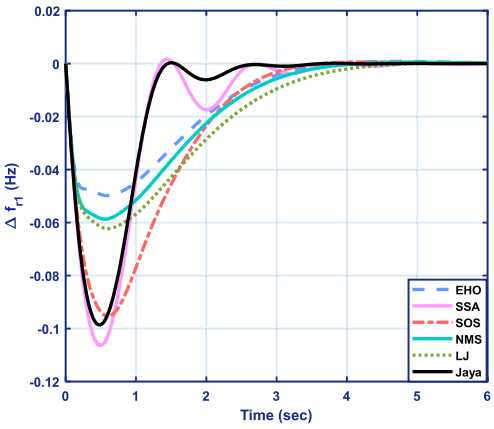

FIGURE 17. Δf_{r1} for case 5.

different. This null hypothesis is put to test at a 0.05 level of significance. Table 10 shows p-value, Q-value, and mean ranks of suggested algorithms determined using the Friedman rank test. According to Table 10, Jaya has a mean rank of 1, whereas EHO, SSA, SOS, NMS, and LJ have mean ranks of 4.8333, 3.8333, 3.5, 3.5, 4.3333, and 1,

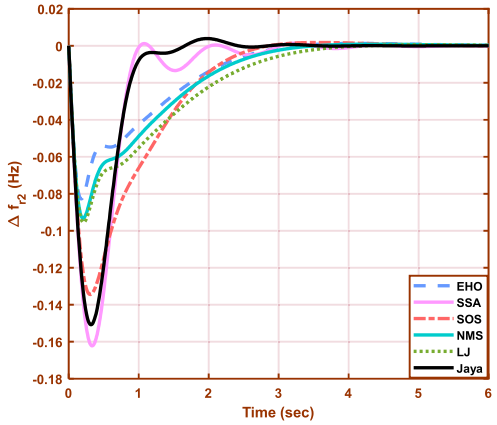

FIGURE 18. Δf_{r2} for case 5.

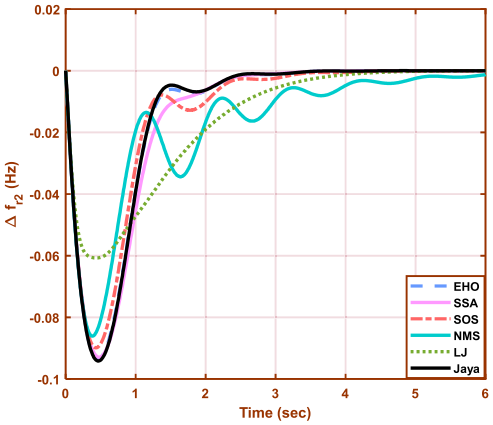

FIGURE 21. Δf_{r2} for case 6.

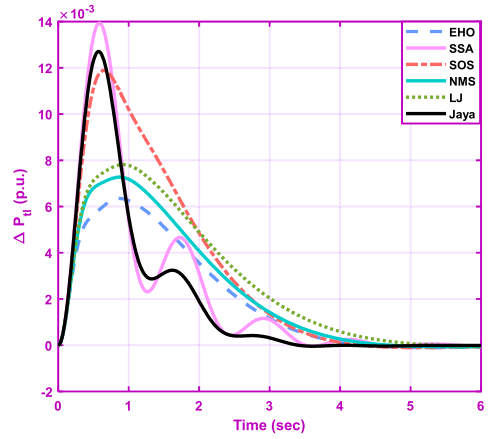

FIGURE 19. ΔP_{tl} for case 5.

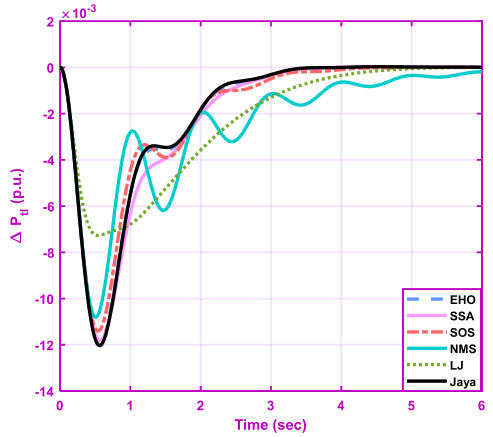

FIGURE 22. ΔP_{tl} for case 6.

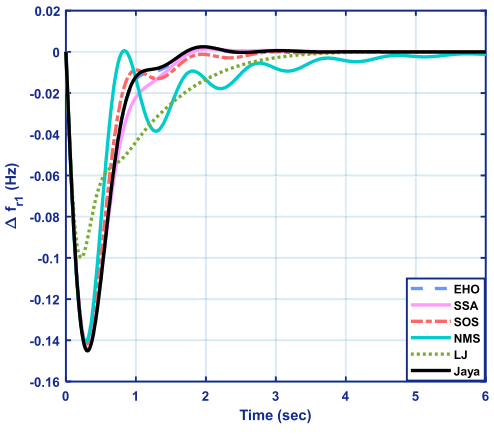

FIGURE 20. Δf_{r1} for case 6.

TABLE 10. Non-parametric statistical analysis.

Friedman rank test						
	EHO	SSA	SOS	NMS	LJ	Jaya
Mean rank	4.8333	3.8333	3.5	3.5	4.3333	1
Q value	$Q = 15.1428$					
p value	$p = 0.0097$					

respectively. In order of performance decrement, the various algorithms are ranked as Jaya, NMS, SOS, SSA, LJ, and EHO using their corresponding mean values. The p value and Q value obtained from this test are 0.0097 and 15.1428, respectively. The obtained p value is substantially lower than 0.05. As a result, the null hypothesis can no longer be accepted. As a consequence of p value, it is clear that results produced using various approaches differ significantly. This demonstrates that Jaya-based PIDm controller outperforms other controllers substantially.

VII. CONCLUSION

This work has proposed a Jaya-based rank exponent method-assisted controller (PIDm) to overcome AGC problems in two-area interconnected power systems. In our approach, three objectives are taken into account, namely integral of time multiplied absolute error (ITAE) for frequency deviations, tie-line power deviation, and area-control errors (ACEs). We have statistically compared the performances of our approach versus state-of-art optimization algorithms, by evaluating standard deviation, lowest, average, and highest

values, to determine the controllers' efficacy and applicability. Controllers tuned with salp swarm algorithm (SSA), Luus-Jaakola (LJ), Nelder-Mead simplex (NMS), symbiotic organisms search (SOS), and elephant herding optimization (EHO) algorithms are compared with our Jaya-based PIDm controller. This analysis has demonstrated the superiority of our method in fitting the given values more closely than the other five state-of-art approaches. Numerical analyses have been carried out under different loading circumstances, including a variety of load fluctuations in interconnected areas.

Future research will be devoted to investigate AGC issues with non-linear models and to understand if other methods other than the rank exponent approach can be fruitfully exploited to solve AGC problems in two-area interconnected power systems.

APPENDIX A
BOUNDARY CONDITIONS

ine Parameter	Min	Max
ϕ_p	0	3
ϕ_i	0	3
ϕ_d	0	3
m	100	500

APPENDIX B
PARAMETERS OF TWO-AREA INTERCONNECTED POWER SYSTEM

Frequency	$f = 60$ Hz;
Frequency bias factors	$\beta_{r1}, \beta_{r2} = 0.05$ p.u. Mw/Hz;
Speed regulating constants for governors	$R_{r1}, R_{r2} = 2.4$ Hz/p.u.;
Time constants for turbine	$T_{t1}, T_{t2} = 0.3$ s;
System gains	$G_{r1}, G_{r2} = 120$ Hz/p.u. Mw;
Torque co-efficient for synchronization	$T_{12} = 0.545$ p.u.;
Area-1 to area-2 tie-line ratio	$A_{12} = -1$.

APPENDIX C
PARAMETERS OF ALGORITHMS

EHO	-
JAYA	-
LJ	$k = 2, \gamma = 0.95$
NMS	$\alpha = 1, \beta = 2, \gamma = 0.5, \delta = 0.5$
SOS	-
SSA	-

REFERENCES

[1] J. Nanda and B. Kaul, "Automatic generation control of an interconnected power system," in *Proc. Inst. Elect. Eng.*, vol. 125, 1978, pp. 385–390.

[2] W. Zhang, W. Sheng, Q. Duan, H. Huang, and X. Yan, "Automatic generation control with virtual synchronous renewables," *J. Modern Power Syst. Clean Energy*, vol. 11, no. 1, pp. 267–279, Jan. 2023.

[3] N. Paliwal, L. Srivastava, and M. Pandit, "Application of grey wolf optimization algorithm for load frequency control in multi-source single area power system," *Evol. Intell.*, vol. 15, no. 1, pp. 563–584, Mar. 2022.

[4] D. Boopathi, K. Jagatheesan, B. Anand, V. Kumarakrishnan, and S. Samanta, "Effect of sustainable energy sources for load frequency control (lfc) of single-area wind power systems," in *Industrial Transformation*. Boca Raton, FL, USA: CRC Press, 2022, pp. 87–98.

[5] Y. Arya, "AGC of two-area electric power systems using optimized fuzzy PID with filter plus double integral controller," *J. Franklin Inst.*, vol. 355, no. 11, pp. 4583–4617, Jul. 2018.

[6] N. Ibraheem and T. S. Bhatti, "AGC of two area power system interconnected by AC/DC links with diverse sources in each area," *Int. J. Electr. Power Energy Syst.*, vol. 55, pp. 297–304, Feb. 2014.

[7] Y. Arya, N. Kumar, and S. K. Gupta, "Optimal automatic generation control of two-area power systems with energy storage units under deregulated environment," *J. Renew. Sustain. Energy*, vol. 9, no. 6, Nov. 2017, Art. no. 064105.

[8] K. Godara, N. Kumar, and K. P. Palawat, "Performance comparison of GA, PSO and WCA for three area interconnected load frequency control system," in *Control and Measurement Applications for Smart Grid*. Cham, Switzerland: Springer, 2022, pp. 373–382.

[9] A. Demiroren, H. L. Zeynelgil, and N. S. Sengor, "The application of ANN technique to load-frequency control for three-area power system," in *Proc. IEEE Porto Power Tech*, Sep. 2001, p. 5.

[10] D. T. Phuong, T. N. Pham, and L. V. Hien, "Exponential stabilization via tracking convergent rate in load frequency control of multi-area power systems with diverse communication delays," *Int. J. Dyn. Control*, vol. 10, no. 1, pp. 107–121, Feb. 2022.

[11] A. Kumar and O. Singh, "Optimal automatic generation control in multi-area power systems with diverse energy sources," in *Advances in Energy Technology*. Cham, Switzerland: Springer, 2022, pp. 289–300.

[12] N. Hakimuddin, A. Khosla, and J. K. Garg, "Centralized and decentralized AGC schemes in 2-area interconnected power system considering multi source power plants in each area," *J. King Saud Univ. Eng. Sci.*, vol. 32, no. 2, pp. 123–132, Feb. 2020.

[13] P. Sanki, M. Basu, and P. S. Pal, "Study of AGC as two area thermal interconnected power system consisting WPG and SPG," in *Proc. Emerg. Trends Electron. Devices Comput. Techn. (EDCT)*, Mar. 2018, pp. 1–6.

[14] P. Sharma, A. Misra, and R. Shankar, "Impact of renewable sources in AGC for two area interconnected power system," in *Proc. Int. Conf. Emerg. Frontiers Electr. Electron. Technol. (ICEFEET)*, Jul. 2020, pp. 1–5.

[15] Y. Boutheina, D. Abdelmoumène, and A. Salem, "AGC of multi-area power systems in presence of HVDC link," in *Proc. Int. Conf. Adv. Electr. Eng. (ICAEE)*, Nov. 2019, pp. 1–5.

[16] P. Dabur, N. K. Yadav, and V. K. Tayal, "MATLAB design and simulation of AGC and AVR for multi area power system and demand side management," *Int. J. Comput. Electr. Eng.*, vol. 3, no. 2, p. 1793, 2011.

[17] E. Çam and I. Kocaarslan, "Load frequency control in two area power systems using fuzzy logic controller," *Energy Convers. Manage.*, vol. 46, no. 2, pp. 233–243, Jan. 2005.

[18] A. Pappachen and A. P. Fathima, "Genetic algorithm based pid controller for a two-area deregulated power system along with dfig unit," in *Proc. IEEE Sponsored 2nd Int. Conf. Innov. Inf., Embedded Commun. Syst. (ICIIECS)*, 2015, pp. 19–20.

[19] L. C. Saikia, J. Nanda, and S. Mishra, "Performance comparison of several classical controllers in AGC for multi-area interconnected thermal system," *Int. J. Electr. Power Energy Syst.*, vol. 33, no. 3, pp. 394–401, Mar. 2011.

[20] E. S. Ali and S. M. Abd-Elazim, "BFOA based design of PID controller for two area load frequency control with nonlinearities," *Int. J. Electr. Power Energy Syst.*, vol. 51, pp. 224–231, Oct. 2013.

[21] K. Jagatheesan, B. Anand, S. Samanta, N. Dey, A. S. Ashour, and V. E. Balas, "Design of a proportional-integral-derivative controller for an automatic generation control of multi-area power thermal systems using firefly algorithm," *IEEE/CAA J. Autom. Sinica*, vol. 6, no. 2, pp. 503–515, Mar. 2019.

[22] I. Nasiruddin, T. S. Bhatti, and N. Hakimuddin, "Automatic generation control in an interconnected power system incorporating diverse source power plants using bacteria foraging optimization technique," *Electr. Power Compon. Syst.*, vol. 43, no. 2, pp. 189–199, Jan. 2015.

[23] H. M. Hasanien, "Whale optimisation algorithm for automatic generation control of interconnected modern power systems including renewable energy sources," *IET Gener., Transmiss. Distrib.*, vol. 12, no. 3, pp. 607–614, Feb. 2018.

[24] R. K. Sahu, S. Panda, and G. T. Chandra Sekhar, "A novel hybrid PSO-PS optimized fuzzy PI controller for AGC in multi area interconnected power systems," *Int. J. Electr. Power Energy Syst.*, vol. 64, pp. 880–893, Jan. 2015.

[25] K. Ullah, A. Basit, Z. Ullah, S. Aslam, and H. Herodotou, "Automatic generation control strategies in conventional and modern power systems: A comprehensive overview," *Energies*, vol. 14, no. 9, p. 2376, Apr. 2021.
[26] Y. L. Abdel-Magid and M. M. Dawoud, "Optimal AGC tuning with genetic algorithms," *Electric Power Syst. Res.*, vol. 38, no. 3, pp. 231–238, Sep. 1996.
[27] N. Pathak, T. S. Bhatti, A. Verma, and I. Nasiruddin, "AGC of two area power system based on different power output control strategies of thermal power generation," *IEEE Trans. Power Syst.*, vol. 33, no. 2, pp. 2040–2052, Mar. 2018.
[28] P. J. Krishna, V. P. Meena, V. P. Singh, and B. Khan, "Rank-sum-weight method based systematic determination of weights for controller tuning for automatic generation control," *IEEE Access*, vol. 10, pp. 68161–68174, 2022.
[29] V. Kumar, U. Prasad, and S. R. Mohanty, "Entirely coupled recurrent neural network-based backstepping control for global stability of power system networks," *IEEE Trans. Autom. Sci. Eng.*, early access, Feb. 14, 2023, doi: 10.1109/TASE.2023.3243405.
[30] A. Fathollahi, A. Kargar, and S. Yaser Derakhshandeh, "Enhancement of power system transient stability and voltage regulation performance with decentralized synergetic TCSC controller," *Int. J. Electr. Power Energy Syst.*, vol. 135, Feb. 2022, Art. no. 107533.
[31] A. Fathollahi and B. Andresen, "Multi-machine power system transient stability enhancement utilizing a fractional order-based nonlinear stabilizer," *Fractal Fractional*, vol. 7, no. 11, p. 808, Nov. 2023.
[32] A. Fathollahi, M. Gheisarnejad, B. Andresen, H. Farsizadeh, and M.-H. Khooban, "Robust artificial intelligence controller for stabilization of full-bridge converters feeding constant power loads," *IEEE Trans. Circuits Syst. II, Exp. Briefs*, vol. 70, no. 9, pp. 3504–3508, Sep. 2023.
[33] B. Yildirim, P. Razmi, A. Fathollahi, M. Gheisarnejad, and M. H. Khooban, "Neuromorphic deep learning frequency regulation in stand-alone microgrids," *Appl. Soft Comput.*, vol. 144, Sep. 2023, Art. no. 110418.
[34] G. Zhang, W. Hu, J. Zhao, D. Cao, Z. Chen, and F. Blaabjerg, "A novel deep reinforcement learning enabled multi-band PSS for multi-mode oscillation control," *IEEE Trans. Power Syst.*, vol. 36, no. 4, pp. 3794–3797, Jul. 2021.
[35] H. O. Bansal, R. Sharma, and P. R. Shreeraman, "PID controller tuning techniques: A review," *J. Control Eng. Technol.*, vol. 2, pp. 168–176, May 2012.
[36] H.-L. Bui and Q.-C. Tran, "A new approach for tuning control rule based on Hedge algebras theory and application in structural vibration control," *J. Vibrat. Control*, vol. 27, nos. 23–24, pp. 2686–2700, Dec. 2021.
[37] S. B. Joseph, E. G. Dada, A. Abidemi, D. O. Oyewola, and B. M. Khammas, "Metaheuristic algorithms for PID controller parameters tuning: Review, approaches and open problems," *Heliyon*, vol. 8, no. 5, May 2022, Art. no. e09399.
[38] R. P. Borase, D. K. Maghade, S. Y. Sondkar, and S. N. Pawar, "A review of PID control, tuning methods and applications," *Int. J. Dyn. Control*, vol. 9, no. 2, pp. 818–827, Jun. 2021.
[39] M. H. K. Roni, M. S. Rana, H. R. Pota, M. M. Hasan, and M. S. Hussain, "Recent trends in bio-inspired meta-heuristic optimization techniques in control applications for electrical systems: A review," *Int. J. Dyn. Control*, vol. 10, no. 3, pp. 999–1011, Jun. 2022.
[40] R. Singh and I. Sen, "Tuning of PID controller based AGC system using genetic algorithms," in *Proc. IEEE Region 10 Conf. TENCON*, Nov. 2004, pp. 531–534.
[41] J. Nanda, S. Mishra, and L. C. Saikia, "Maiden application of bacterial foraging-based optimization technique in multiarea automatic generation control," *IEEE Trans. Power Syst.*, vol. 24, no. 2, pp. 602–609, May 2009.
[42] R. K. Sahu, S. Panda, and S. Padhan, "Optimal gravitational search algorithm for automatic generation control of interconnected power systems," *Ain Shams Eng. J.*, vol. 5, no. 3, pp. 721–733, Sep. 2014.
[43] P. Mohanty, R. K. Sahu, and S. Panda, "A novel hybrid many optimizing liaisons gravitational search algorithm approach for AGC of power systems," *Automatika*, vol. 61, no. 1, pp. 158–178, Jan. 2020.
[44] V. P. Meena, U. K. Yadav, A. Gupta, and V. P. Singh, "Reduced-order model based design of PID control for zeta converter using GWO algorithm," in *Proc. IEEE Int. Conf. Power Electron., Drives Energy Syst. (PEDES)*, Dec. 2022, pp. 1–5.
[45] V. P. Meena, H. Jangid, and V. P. Singh, "GWO based reduced-order modeling of Doha water treatment plant," in *Proc. Int. Conf. Control, Autom., Power Signal Process. (CAPS)*, Dec. 2021, pp. 1–5.
[46] P. D. Dewangan, N. Patnana, L. Barik, P. J. Krishna, V. P. Meena, and V. P. Singh, "Performance evaluation of GWO algorithm using different initialization strategies," in *Proc. 8th Int. Conf. Adv. Comput. Commun. Syst. (ICACCS)*, vol. 1, Mar. 2022, pp. 714–718.
[47] S. M. Abd-Elazim and E. S. Ali, "Load frequency controller design via BAT algorithm for nonlinear interconnected power system," *Int. J. Electr. Power Energy Syst.*, vol. 77, pp. 166–177, May 2016.
[48] S. S. Pati, A. Behera, and T. K. Panigrahi, "Automatic generation control of multi-area system incorporating renewable unit and energy storage by bat algorithm," in *Innovative Product Design and Intelligent Manufacturing Systems*. Cham, Switzerland: Springer, 2020, pp. 713–722.
[49] P. C. Pradhan, R. K. Sahu, and S. Panda, "Firefly algorithm optimized fuzzy PID controller for AGC of multi-area multi-source power systems with UPFC and SMES," *Eng. Sci. Technol., Int. J.*, vol. 19, no. 1, pp. 338–354, Mar. 2016.
[50] R. Poli, J. Kennedy, and T. Blackwell, "Particle swarm optimization: An overview," *Swarm Intell.*, vol. 1, no. 1, pp. 33–57, 2007.
[51] V. Kumarakrishnan, G. Vijayakumar, D. Boopathi, K. Jagatheesan, S. Saravanan, and B. Anand, "Frequency regulation of interconnected power generating system using ant colony optimization technique tuned pid controller," in *Control and Measurement Applications for Smart Grid*. Cham, Switzerland: Springer, 2022, pp. 129–141.
[52] K. Naidu, H. Mokhlis, A. H. A. Bakar, and V. Terzija, "Performance investigation of ABC algorithm in multi-area power system with multiple interconnected generators," *Appl. Soft Comput.*, vol. 57, pp. 436–451, Aug. 2017.
[53] S. P. Singh, T. Prakash, V. P. Singh, and M. G. Babu, "Analytic hierarchy process based automatic generation control of multi-area interconnected power system using Jaya algorithm," *Eng. Appl. Artif. Intell.*, vol. 60, pp. 35–44, Apr. 2017.
[54] V. P. Meena and V. P. Singh, "Design of FOPID controller for riverol-pilipovik water treatment plant exploiting Jaya algorithm," in *Proc. Int. Conf. Comput., Electron. Electr. Eng. their Appl. (IC2E)*, Jun. 2023, pp. 1–5.
[55] R. K. Sahu, T. S. Gorripotu, and S. Panda, "Automatic generation control of multi-area power systems with diverse energy sources using teaching learning based optimization algorithm," *Eng. Sci. Technol., Int. J.*, vol. 19, no. 1, pp. 113–134, Mar. 2016.
[56] V. P. Meena, A. V. Waghmare, and V. P. Singh, "Reduced-order modelling of level-up DC–DC converter using TLBO algorithm," in *Proc. IEEE 3rd Int. Conf. Sustain. Energy Future Electr. Transp. (SEFET)*, Aug. 2023, pp. 1–6.
[57] E. S. Ali and S. M. Abd-Elazim, "Bacteria foraging optimization algorithm based load frequency controller for interconnected power system," *Int. J. Electr. Power Energy Syst.*, vol. 33, no. 3, pp. 633–638, Mar. 2011.
[58] K. J. Åström and T. Hägglund, "The future of PID control," *Control Eng. Pract.*, vol. 9, no. 11, pp. 1163–1175, Nov. 2001.
[59] M. A. Johnson and M. H. Moradi, *PID Control*. Cham, Switzerland: Springer, 2005.
[60] E. Roszkowska, "Rank ordering criteria weighting methods—A comparative overview," *Optimum. Studia Ekonomiczne*, vol. 5, no. 65, pp. 14–33, 2013.
[61] N. Gupta Gourisetti, M. Mylrea, and H. Patangia, "Application of rank-weight methods to blockchain cybersecurity vulnerability assessment framework," in *Proc. IEEE 9th Annu. Comput. Commun. Workshop Conf. (CCWC)*, Jan. 2019, pp. 0206–0213.
[62] P. Sureeyatanapas, "Comparison of rank-based weighting methods for multi-criteria decision making," *Eng. Appl. Sci. Res.*, vol. 43, pp. 376–379, Nov. 2016.
[63] R. V. Rao, "Jaya: A simple and new optimization algorithm for solving constrained and unconstrained optimization problems," *Int. J. Ind. Eng. Comput.*, vol. 7, no. 1, pp. 19–34, 2016.
[64] K. Abhishek, V. R. Kumar, S. Datta, and S. S. Mahapatra, "Application of Jaya algorithm for the optimization of machining performance characteristics during the turning of CFRP (epoxy) composites: Comparison with TLBO, GA, and ICA," *Eng. With Comput.*, vol. 33, no. 3, pp. 457–475, Jul. 2017.
[65] A. A. Khan, V. P. Meena, A. V. Waghmare, U. K. Yadav, and V. P. Singh, "Elephant herding optimization assisted reduction of level-up DC–DC converter," in *Proc. IEEE 3rd Int. Conf. Sustain. Energy Future Electric Transp. (SEFET)*, Aug. 2023, pp. 1–6.

[66] V. Meena, L. Barik, and V. Singh, "Luus–Jaakola algorithm assisted reduced-order model of interval modeling Doha water treatment plant," in *Proc. AIP Conf.*, vol. 2705, 2023, Art. no. 040009.
[67] J. Derrac, S. García, D. Molina, and F. Herrera, "A practical tutorial on the use of nonparametric statistical tests as a methodology for comparing evolutionary and swarm intelligence algorithms," *Swarm Evol. Comput.*, vol. 1, no. 1, pp. 3–18, Mar. 2011.

MAMTA (Student Member, IEEE) was born in Jhunjhunu, Rajasthan, India, in July 1996. She received the B.Tech. degree in electrical engineering from the Bhartiya Institute of Engineering & Technology, Sikar, Rajasthan, in 2016. She is currently pursuing the M.Tech. degree in power systems engineering with the Malaviya National Institute of Technology Jaipur, Jaipur, India. Her research interests include power system optimization and control systems.

V. P. SINGH (Senior Member, IEEE) received the B.Tech. degree (Hons.) in electrical engineering from Uttar Pradesh Technical University, Lucknow, India, in 2007, and the M.Tech. degree in control and instrumentation and the Ph.D. degree in electrical engineering from the Motilal Nehru National Institute of Technology, Allahabad, India, in 2009 and 2013, respectively. He has been an Assistant Professor with the Malaviya National Institute of Technology Jaipur, India, since 2019. He was with the National Institute of Technology, Raipur, as an Assistant Professor, from 2013 to 2019. He has published several articles in international and national journals and conferences. His research interests include system modeling, model order reduction, and applications of optimization. He is a Faculty Advisor of IEEE Student Branch with the Malaviya National Institute of Technology Jaipur. During his tenure as a Faculty Advisor, he established five new IEEE student chapters and organized 17 guest lectures from IEEE student chapters. Along with these, he is currently holding a Faculty Advisor of IEEE Systems, Man and Cybernetics Society, IEEE Systems Council, and IEEE Council on Electronic Design Automation.

AKANKSHA V. WAGHMARE (Student Member, IEEE) received the B.E. degree in electrical (electronics and power) engineering from the Shri Sant Gajanan Maharaj College of Engineering (SSGMCE), Shegaon, Maharashtra, India, in 2019, and the M.Tech. degree in energy systems engineering from the National Institute of Technology (NIT), Jamshedpur, India, in 2022. She is currently pursuing the Ph.D. degree in electrical engineering with the Malaviya National Institute of Technology (MNIT) Jaipur, India. Her research interests include applications of control systems, power systems, machine learning, and model order reduction.

VEERPRATAP P. MEENA (Member, IEEE) received the B.Tech. degree in electrical engineering from the Government Engineering College, Bikaner, India, in 2018, the M.Tech. degree in power system engineering from Indian Institute of Technology Roorkee (IIT Roorkee), in 2020, and the Ph.D. degree in electrical engineering from the Malaviya National Institute of Technology (MNIT) Jaipur, India, in 2023. Currently, he is also a Postdoctoral Fellow with Amrita Vishwa Vidyapeetham, Bengaluru, India, and has been the Chair of IEEE Systems Council Systems Education Technical Committee, USA, since 2023. His research interests include electric vehicles, power systems, system modeling, controller design, interval systems, model order reduction, applications of optimization algorithms, and power electronics. He contributed to the body of knowledge by publishing several research papers in international journals and conferences. Also, he has served as the general chair, the program chair, and a program committee member of several international conferences and workshops. He is an Associate Editor/Editorial Board Member of refereed journals, in particular the IEEE ACCESS and *International Journal of Intelligent Engineering Informatics* (Inderscience).

FRANCESCO BENEDETTO (Senior Member, IEEE) has been the Chair of the IEEE 1900.1 standard "Definitions and Concepts for Dynamic Spectrum Access: Terminology Relating to Emerging Wireless Networks, System Functionality, and Spectrum Management," since 2016. He has been the Leader of the WP 3.5 on "Development of Advanced GPR Data Processing Technique" of the European COST Action TU1208—Civil Engineering Applications of Ground Penetrating Radar. He is an Associate Editor of IEEE ACCESS, an Editor of the IEEE SDN Newsletter, an Associate Editor of the AEÜ—*International Journal of Electronics and Communications* (Elsevier), the Editor-in-Chief of the *Recent Advances on Computer Science and Communications* (Bentham), the General Co-Chair of the IEEE 43rd International Conference on Telecommunications and Signal Processing (TSP 2020), the General Chair of the Series of International Workshops on Signal Processing for Secure Communications (SP4SC 2014, 2015, and 2016), and the Lead Guest Editor of the Special Issue on "Advanced Ground Penetrating Radar Signal Processing Techniques" for the *Signal Processing* journal (Elsevier). He also served as a reviewer for several IEEE TRANSACTIONS, IET proceedings, EURASIP, and Elsevier journals; and a TPC member for several IEEE international conferences and symposia in the same fields.

TARUN VARSHNEY (Senior Member, IEEE) received the B.E. degree in electronics and instrumentation engineering from Rajasthan University, Jaipur, India, in 2001, the M.Tech. degree in control and instrumentation from MNNIT, Allahabad, India, in 2007, and the Ph.D. degree from MNNIT Allahabad in 2014. Currently, he is the Head of the Department and a Professor with the Department of Electrical, Electronics and Communication Engineering, SET, Sharda University, Greater Noida, Uttar Pradesh, India. His research interests include intelligent control systems, multi-variable systems modelling, and neural networks. He is a reviewer of SCI, E-SCI, and Scopus indexed journals. He is a Life Member of ISTE, a member of ISA, and a fellow of IE(I).

Open Access funding provided by 'Università degli Studi Roma Tre' within the CRUI CARE Agreement